The Human Bone–Oxidized Titanium Implant Interface: A Light Microscopic, Scanning Electron Microscopic, Back-Scatter Scanning Electron Microscopic, and Energy-Dispersive X-Ray Study of Clinically Retrieved Dental Implants

Peter Schüpbach, PhD;* Roland Glauser, DDS;† Antonio Rocci, DDS;‡ Massimiliano Martignoni, DDS;§ Lars Sennerby, DDS, PhD;‖ AnnaKarin Lundgren, DDS, PhD;‖ Jan Gottlow, DDS, PhD‡‖

ABSTRACT

Background: Surface modification of titanium implants by anodic oxidation may lead to enhanced bone integration. For instance, in vivo studies have demonstrated formation of more bone contacts in less time than for turned control implants. In addition, oxidized implants have shown a higher resistance to torque forces, indicating a strong interlock between bone and the oxide layer. However, the structure of the oxidized titanium-bone interface in high resolution is not known.

Purpose: The aim of the study was to analyze the human bone–oxidized titanium interface at a high-resolution level. Of particular interest was the relationship between bone tissue and the pores of the surface oxide.

Materials and Methods: Twelve clinically retrieved implants with an oxidized surface (TiUnite™, Nobel Biocare AB, Göteborg, Sweden) were used. Seven were regular dental implants and five were experimental mini-implants and had been subjected to immediate, early, or no loading. They were retrieved after 5 to 9 months of healing and were processed and analyzed using light microscopy, scanning electron microscopy (SEM) in normal and back-scatter (BS-SEM) modes, and energy-dispersive x-ray (EDX) analysis techniques.

Results: Bone formation was observed to occur from adjacent bone structures toward the implant surface, and it was evident that bone formation had occurred at the implant surface. SEM, BS-SEM, and EDX revealed that mineralized bone had grown into the pores of the surface oxide layer, including pores with small diameters (< 2 μm).

Conclusions: The clinically retrieved oxidized implants showed evidence of bone growth into the pores of the surface oxide layer. The findings indicate the establishment of a strong interlock between the bone and the oxidized titanium implant, which is suggested to be beneficial for clinical performance.

KEY WORDS: anodic oxidation, back-scatter scanning electron microscopy, energy-dispersive x-ray, histology, scanning electron microscopy, titanium implants

The use of turned titanium implants ad modum Brånemark as anchorage units for dental prostheses has been documented in clinical follow-up studies as a predictable treatment procedure.[1] However, clinical evidence indicates that in demanding situations, such as implantation into sites of poor bone quality or quantity, irradiated or grafted bone, or smokers, or the use of short implants in combination with high loads may lead to higher failure rates.[2] From a structural and morphologic point of view, this means difficulties in establishing and maintaining direct bone-implant contact during healing and functional loading.

Ultrastructural studies of machined implants have indicated that bone and titanium are not continuous at the bone-titanium interface but are separated by one or

*Peter Schüpbach Ltd, Laboratory for Microscopic Analysis, Horgen, Switzerland; †Department for Fixed Prosthodontics and Dental Materials, University of Zurich, Zurich, Switzerland; ‡private practice, Chieti, Italy; §private practice, Rome, Italy; ‖Department of Biomaterials, Institute for Surgical Sciences, Sahlgrenska Academy, University of Göteborg, Göteborg, Sweden

Reprint requests: Peter Schüpbach, PhD, Peter Schupbach Ltd, Laboratory for Microscopic Analysis, Zugerstrasse 64, CH-8810 Horgen, Switzerland; e-mail: pmsch@bluewin.ch

two layers about 0.1 to 0.5 μm wide.[3] The literature is not conclusive with regard to the structure and contents of the layers, but cement line–like and amorphous layers have been described.[3] In spite of this, the implants become firmly anchored in bone and show an increased resistance to torque and bending forces with time.[4,5] One explanation could be interlocking owing to ingrowth of bone into larger surface irregularities. Many research teams have investigated bone response to various surface treatments, which results in a changed surface topography and, in many instances, to an increased roughness and an enlarged surface area.[6] Experimental studies have shown more rapid formation of bone contacts and higher amounts of bone contacts in parallel with higher resistance to torque forces compared with nonmodified control implants.[7–10] It can be speculated that the changed surface topography facilitates cellular migration and differentiation at the tissue-implant interface[11] and that formation and ingrowth of bone into surface irregularities result in a stronger integration of the implant, which may be beneficial in the clinical situations mentioned above.

Anodic oxidation is one technique for surface modification of titanium and results in an increased thickness of the native oxide layer and a changed surface topography.[12,13] The thickened titanium oxide layer is highly crystalline, containing anatase and rutile, which are the most common crystalline forms of titanium oxide, and phosphates.[12] The most striking characteristic is the formation of interconnecting pores, which are from less than 1 to 10 μm wide. Histologic studies of biopsies from humans and animals have shown a high affinity of bone to the surface of oxidized implants.[14–18] However, the structure of the bone–oxidized implant interface at high resolution is not known.

The aim of this investigation was to analyze the human bone–oxidized titanium implant interface at a high-resolution level using light microscopy, scanning electron microscopy (SEM), back-scatter electron microscopy (BS-SEM), and energy-dispersive x-ray (EDX) analysis techniques.

MATERIAL AND METHODS

Ethical Considerations

The patients presented themselves for implant treatment and subsequently volunteered to have extra implants inserted in the posterior mandible or maxilla for the purpose of histologic research. The study was conducted in accordance with the Declaration of Helsinki. All subjects gave their written, informed consent prior to participation. They all had the right to withdraw from the study at any time without jeopardizing their ordinary treatment. The study was approved by the regional ethical committee at the University of Zürich, Switzerland.

Implants

Twelve clinically retrieved implants were used for histologic analyses in the present study:

1. Six regular dental implants (TiUnite™, Regular Platform Mk III and Regular Platform Mk IV, Brånemark System®, Nobel Biocare AB, Göteborg, Sweden) from a previous light microscopic study in which the study design and clinical circumstances were described in detail.[18] In brief, nine implants were placed in the posterior mandible of five patients and were subjected to immediate loading ($n = 2$) or early loading after 2 months ($n = 7$).
2. One Nobel Perfect™ implant (Nobel Biocare AB) retrieved from the maxilla of one patient after 6 months of loading.
3. Five nonloaded mini-implants (ø 2.3 mm, length 5 mm) with an oxidized surface (TiUnite) retrieved after 4 to 8 months in five patients were used.
4. One unused oxidized implant (TiUnite, Regular Platform Mk III).

Light Microscopy

All biopsies were fixed in 4% buffered formaldehyde. The specimens were dehydrated in a series of ethanol and were embedded in Technovit 7200 VLC (Heraeus Kulzer GmbH & Co., Wehrheim, Germany). Ground sections were prepared using sawing and grinding techniques (Exakt Apparatebau, Norderstedt, Germany).[19] The sections were ground to a final thickness of about 20 μm and were stained with toluidine blue O and pyronin G. The slides were viewed and photographed with a Leica DM4000 (Leica, Glattbrugg, Switzerland) light microscope, equipped with a Leica DFC480 high-resolution video camera.

Scanning Electron Microscopy

Specimens for SEM were washed with a 0.185 M Na-cacodylate buffer (pH = 7.4; 346 mOsm). In some small areas, bone was carefully broken away from the implant

surface using small tweezers and scalpels to expose the implant-bone interface. The specimens were then dehydrated in ascending grades of acetone and dried in a critical point apparatus using carbon dioxide as the transitory fluid. The specimens were sputter-coated with gold and examined in a Cambridge Stereoscan S-180 (Cambridge Instruments, Dortmund, Germany).

Back-Scatter Scanning Electron Microscopy

For BS-SEM, ground sections through the implants were highly polished using different grades of diamond-coated papers and a 0.25 μm diamond paste (DP-paste, Struers, Ballerup, Denmark). The sections were mounted on holders and 6 nm sputter-coated with carbon by means of a MED 020 sputter device (Bal-Tec, Liechtenstein). In a Cambridge Stereoscan S-180 SEM (Cambridge Instruments), back-scatter imaging was used to demonstrate the degree of mineralization.

EDX Analysis

For EDX analysis, ground sections were mounted on holders and 6 nm sputter-coated with carbon by means of a MED 020 sputter device (Bal-Tec). In a Philips scanning- and transmission electron microscope (Philips, Eindhoven, the Netherlands), EDX analyses were performed at 5 and 10 kV.

RESULTS

Light Microscopic Analyses

Light microscopy showed similar bone morphology around and at the implants in spite of different time periods between placement and retrieval. Light microscopy of ground sections viewed in both transmitted light (Figure 1) and polarized light (Figure 2) revealed the intimate contact of the newly formed bone with the oxidized implant surface. It was obvious that the integration process occurred by growth from adjacent bone surfaces toward the surface (distance osteogenesis) and by bone formation directly on the surface oxide (contact osteogenesis). The former was characterized by apposition of bone at the wound edges of existing bone, with successive layers of bone being formed toward the implant surface (Figure 3). Bone formation directly on the oxidized implant surface was often manifested as a narrow zone of bone that followed the contour of the implant (Figure 4). The front of the thin rims and the surface facing the tissues were often occupied by active

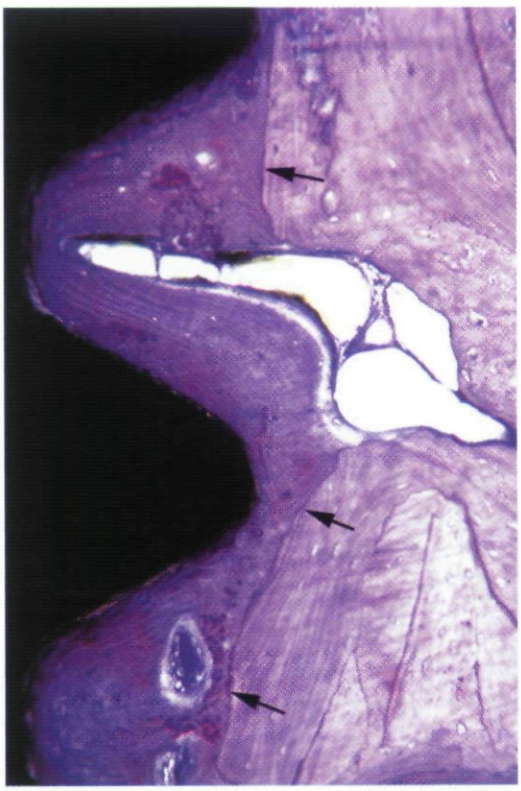

Figure 1 Final osseointegration. Note the border of local bone (*arrows*). Ground section (×20 original magnification; stained with toluidine).

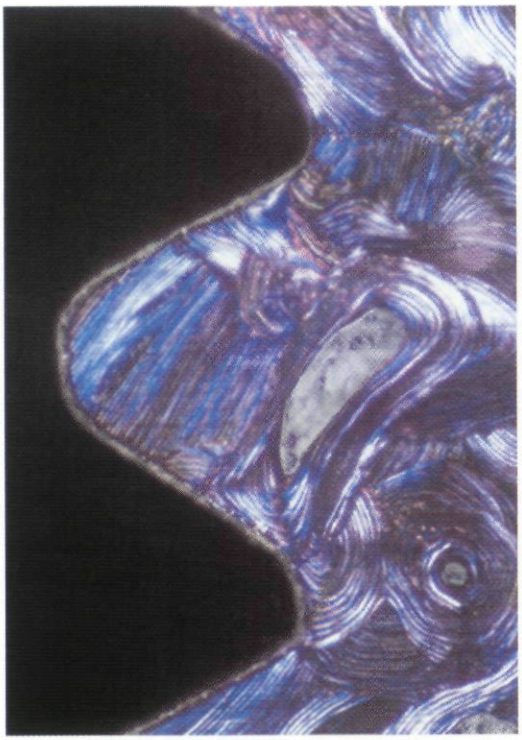

Figure 2 Final osseointegration. Note the presence of the oxide layer between the body of the implant and bone. Ground section; polarized light microscopy (×20 original magnification; stained with toluidine blue).

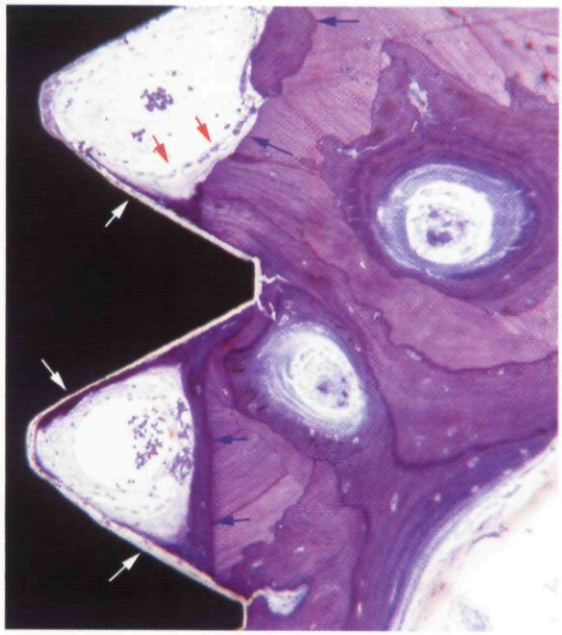

Figure 3 Light microscopic view of bone formation by contact osteogenesis along two threads of an oxidized implant surface (*white arrows*). Note the border of local bone (*blue arrows*) and the presence of osteoblasts (*red arrows*). Ground section (×20 original magnification; stained with toluidine blue).

osteoblasts and osteoid. Signs of cell migration from the marrow tissue to the mineralizing fronts could be seen in higher magnification, indicating recruitment and differentiation of immature cells to preosteoblasts and osteoblasts (Figure 5).

SEM Analyses

SEM evaluation of the unused oxidized implant demonstrated a porous surface texture with both micropores of between 1 and 7 μm in diameter and nanopores with orifices of less than 1 μm (Figure 6).

SEM micrograph of retrieved implants showed bone tissue in the micropores of the oxide layer (Figure 7). The ingrowth and anchorage of bone were independent of the pore size, and bone was also present in pores with a diameter of less than 1 μm (Figure 8). The presence of bone in the pores was confirmed by EDX. EDX analysis of the bone-implant interface showed high peaks for titanium, calcium, and phosphorus (Figure 9).

The combination of EDX and SEM revealed that new bone was integrated into the implant surface. Analysis

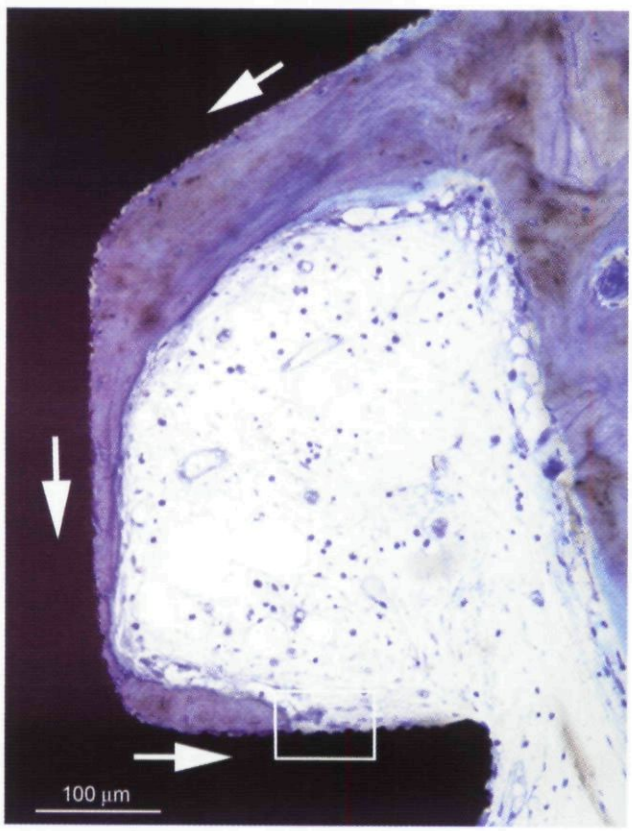

Figure 4 View of bone formation along an oxidized implant surface using light microscopy. Note the direction of bone formation (*arrows*). The area outlined showing the advancing front of bone formation is magnified in Figure 5. Ground section (stained with toluidine blue).

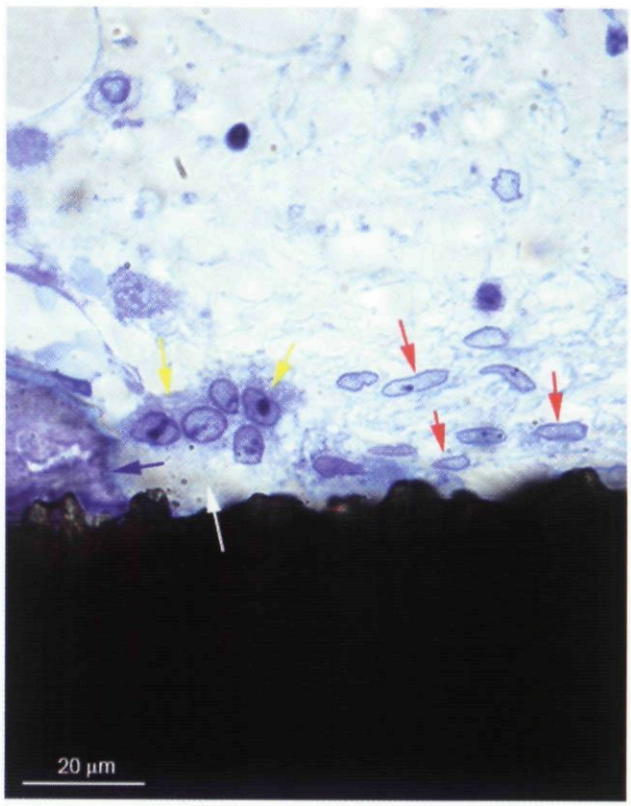

Figure 5 Higher magnification view of the area outlined in Figure 4 using light microscopy showing the advancing front of bone formation. Note the population of both preosteoblasts (*red arrows*) and osteoblasts (*yellow arrows*). Also note the presence of the osteoid (*white arrow*) and the front of mineralization (*blue arrow*). Ground section (stained with toluidine blue).

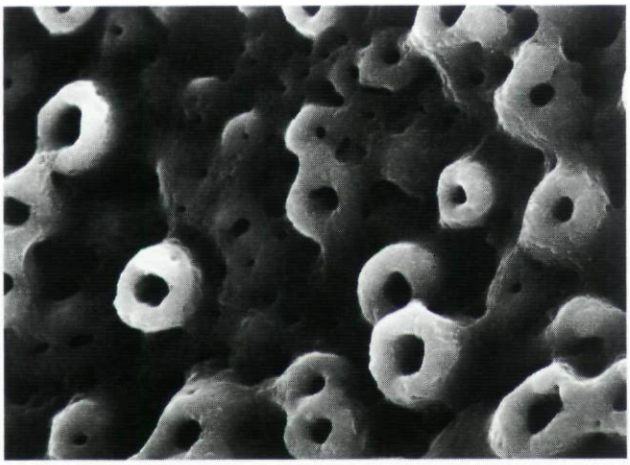

Figure 6 Scanning electron micrograph of a porous oxidized surface. Note the presence of both nanopores with diameters less than 1 μm and micropores with diameters ranging between 1 and 7 μm. (×1400 original magnification).

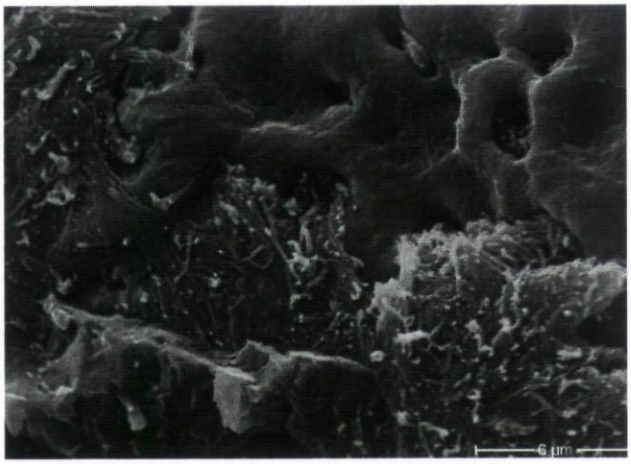

Figure 7 Scanning electron micrograph showing the bone-implant interface. Bone was broken away to expose the implant surface. Note the presence of bone anchored in the orifices of the pores.

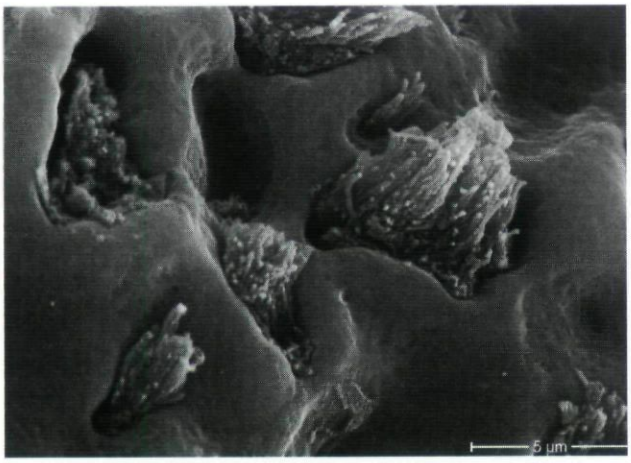

Figure 8 Scanning electron micrograph showing bone anchored in the orifice of a nanopore.

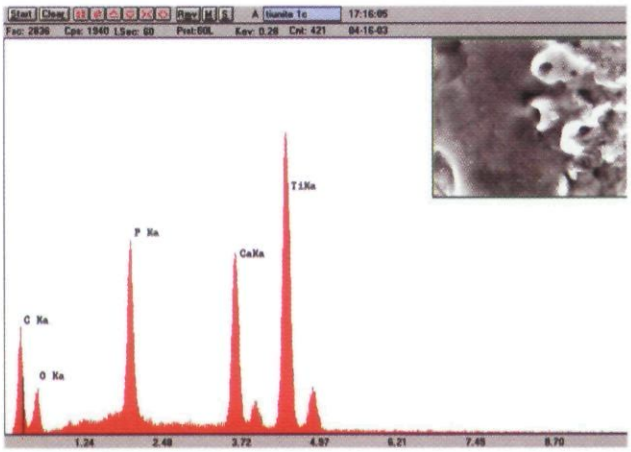

Figure 9 Energy-dispersive x-ray analysis of the interface between the oxide layer and bone. Note the large peaks for titanium, calcium, and phosphorus.

showing the distribution of the individual elements showed the presence of titanium in the titanium oxide layer and the presence of calcium and phosphorus in the adjacent tissue. Phosphorus was also present in the oxidized layer (Figure 10). Digitally composed images produced by superimposing the four individual images presented in Figure 10 show the presence of bone in intimate contact with the oxidized implant surface (Figure 11). Using the same technique, bone was also observed in the orifices of the pores (Figure 12) and extending down to the very bottom of the pores (Figure 13).

Ground sections examined under BS-SEM confirmed the intimate contact of bone with the oxide layer (Figure 14) and the presence of bone in the pores (Figure 15).

DISCUSSION

The present study showed a positive tissue response to clinically retrieved oxidized titanium implants, resulting in intimate contact between mineralized bone tissue and the surface layer, which is in line with previous light microscopic investigations.[13–18] Apart from ingrowth from adjacent bone surfaces, it was obvious that bone formation also occurred directly on the surface. The high-resolution analyses with SEM, BS-SEM, and EDX revealed that the newly formed bone extended into the pores of the surface layer. The findings suggest a strong interlock between the bone tissue and the implant surface, with no detectable differences between unloaded, early loaded, and immediately loaded implants.

Previously published studies have suggested an optimal pore size for bone ingrowth in the range of 50

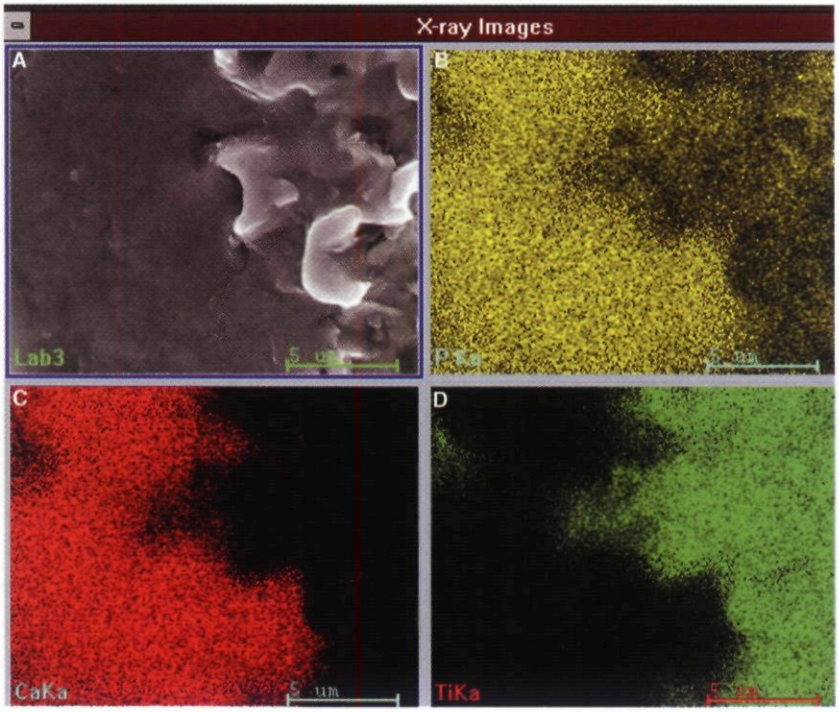

Figure 10 *A–D*, Energy-dispersive x-ray analysis showing the interface between the oxide layer and bone (*A*). Note the presence of phosphorus (*B*) and calcium (*C*) in the adjacent mineralized bone and the presence of titanium (*D*) restricted to the implant.

to around 400 μm.[20,21] Based on the findings of the present study, it is, however, clear that bone can be formed into smaller pores with diameters of less than 2 μm. One possible explanation, supported by the evidence provided by this study, is that it is not necessary for osteoblasts to enter into the pores to form bone. Osteoblasts are polarized cells, and the findings of the present investigation indicate that these cells stay at the surface and deposit bone matrix into the pores of the oxidized surface. The background mechanisms for the affinity of bone to the pores are not known. The bone formation process includes a complex interplay between different substances released from cells and vessels. It can be speculated that the porous surface acted as a reservoir for such factors, which, in turn, had chemotactic effects on cells during healing. Moreover, the tita-

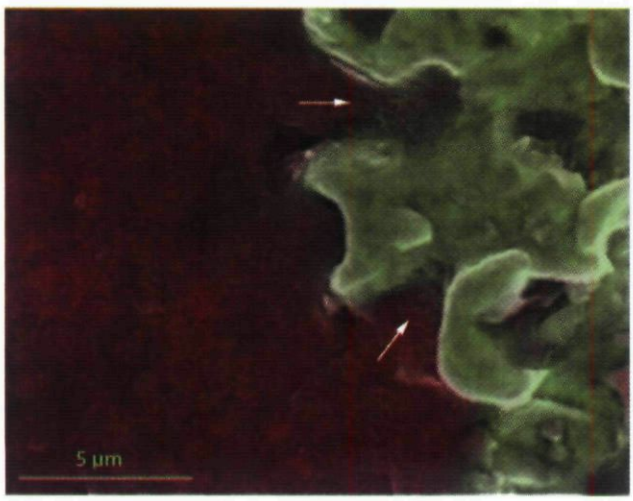

Figure 11 Composite image produced by superimposing the images in Figure 10, A–D. Note the intimate contact of bone with the oxide layer (*arrows*). Scanning electron microscopic–analysis, composite image.

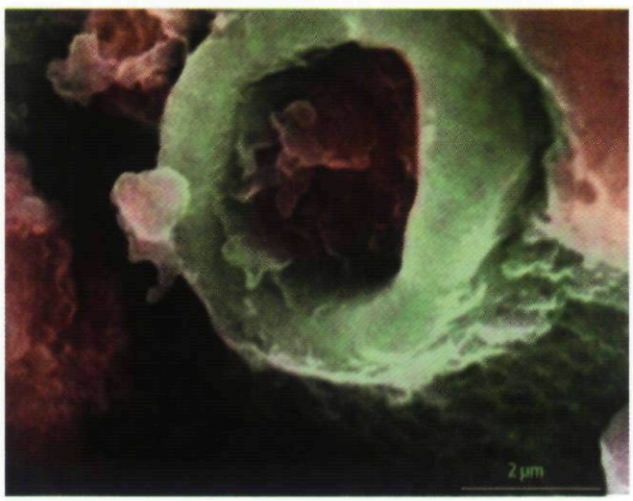

Figure 12 Composite image produced by superimposing the images in Figure 10, A–D. Note the presence of mineralized bone in a pore. Scanning electron microscopic–energy-dispersive x-ray analysis.

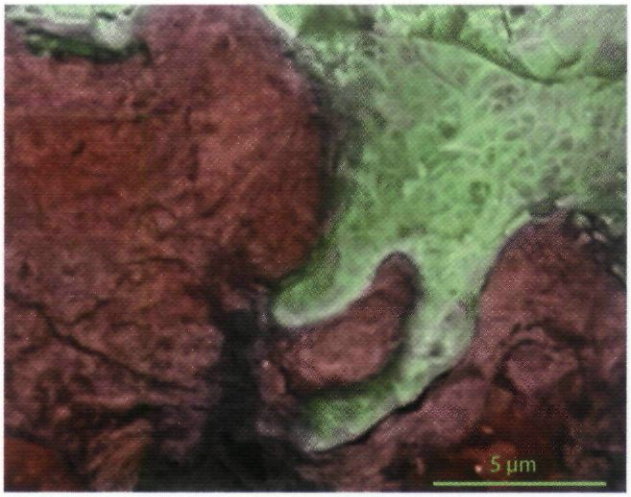

Figure 13 Composite image produced by superimposing the images in Figure 10, A–D. Note the presence of mineralized bone extending to the bottom of a pore. Scanning electron microscopic–energy-dispersive x-ray analysis.

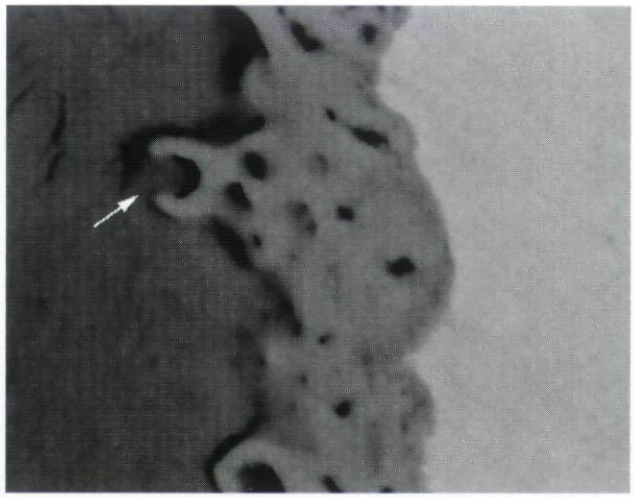

Figure 15 Back-scattered scanning electron microscopic view of a cross-section through the oxide layer-one interface. Note the presence of bone in an open pore (*arrow*). Ground section.

nium oxide itself could have promoted mineralization owing to its ability to bind calcium and thereby stimulate bone formation.[22]

The surface analyzed in the present study has been in clinical use for about 5 years. Clinical follow-up studies have shown good clinical results, also when used for immediate loading with up to 4 years of follow-up.[23–26] Some studies indicate better results with the oxidized surface in comparison with turned implants. A prospective randomized clinical study by Rocci and colleagues found a 10% higher survival rate following immediate loading of oxidized implants in the posterior mandible compared with the outcome of machined implants (95.5% and 85.5%, respectively; $p = .0575$).[27] Glauser and colleagues performed two prospective clinical studies on immediate loading using oxidized implants[24] and turned implants.[28] They reported a failure rate of 3% for oxidized implants and 17.3% for turned implants. Although these were two separate studies, the results indicate a difference. Comparative studies are needed to statistically evaluate possible differences.

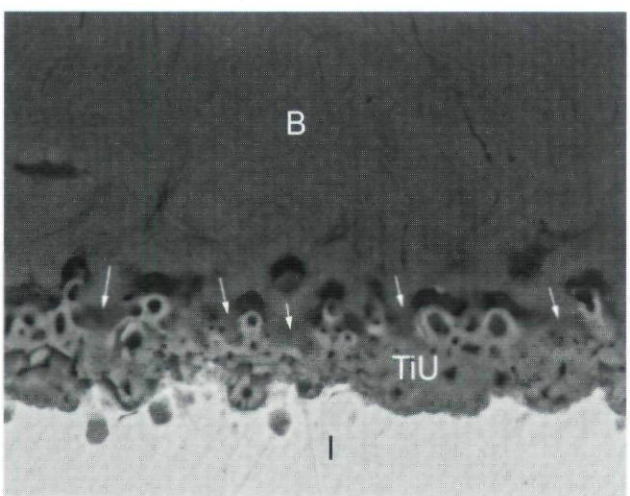

Figure 14 Back-scattered scanning electron microscopic view of a cross-section through the oxide layer-one interface. Note the intimate interlinkage between bone and oxide layer (*arrows*). B = bone; I = implant; TiU = TiUnite. Ground section.

CONCLUSION

The clinically retrieved oxidized implants showed evidence of bone growth into the pores of the surface oxide layer. The findings indicate the establishment of a strong interlock between the bone and the oxidized titanium implant, which is suggested as being beneficial for clinical performance.

REFERENCES

1. Esposito M, Hirsch JM, Lekholm U, Thomsen P. Biological factors contributing to failures of osseointegrated oral implants.(I). Success criteria and epidemiology. Eur J Oral Sci 1998; 106:527–551.
2. Sennerby L, Roos J. Surgical determinants of clinical success of osseointegrated oral implants: a review of the literature. Int J Prosthodont 1998; 11:408–420.
3. Albrektsson TO, Johansson CB, Sennerby L. Biological aspects of implant dentistry: osseointegration. Periodontology 2000 1994; 4:58–73.
4. Johansson C, Albrektsson T. Integration of screw implants in the rabbit: a 1-year follow-up of removal torque of titanium implants. Int J Oral Maxillofac Implants 1987; 2:69–75.
5. Meredith N, Shagaldi F, Alleyne D, Sennerby L, Cawley P. The application of resonance frequency measurements to

study the stability of titanium implants during healing in the rabbit tibia. Clin Oral Implants Res 1997; 8:234–243.

6. Wennerberg A. On surface roughness and implant incorporation. Göteborg: University of Göteborg, 1996. (Thesis)
7. Carlsson L, Rostlund T, Albrektsson B, Albrektsson T. Removal torques for polished and rough titanium implants. Int J Oral Maxillofac Implants 1988; 3:21–24.
8. Wennerberg A, Albrektsson T, Andersson B, Krol JJ. A histomorphometric and removal torque study of screw-shaped titanium implants with three different surface topographies. Clin Oral Implants Res 1995; 6:24–30.
9. Gotfredsen K, Berglundh T, Lindhe J. Anchorage of titanium implants with different surface characteristics: an experimental study in rabbits. Clin Implant Dent Relat Res 2000; 2:120–128.
10. Li D, Ferguson SJ, Beutler T, et al. Biomechanical comparison of the sandblasted and acid-etched and the machined and acid-etched titanium surface for dental implants. J Biomed Mater Res 2002; 60:325–332.
11. Davies JE. Mechanisms of endosseous integration. Int J Prosthodont 1998; 11:391–401.
12. Hall J, Lausmaa J. Properties of a new porous oxide surface on titanium implants. Appl Osseointegration Res 2000; 1:5–8.
13. Larsson C. The interface between bone and implants with different surface oxide properties. Appl Osseointegration Res 2000; 1:9–14.
14. Albrektsson T, Johansson C, Lundgren AK, Sul Y, Gottlow J. Experimental studies on oxidized implants. A histomorphometrical and biomechanical analysis. Appl Osseointegration Res 2000; 1:21–24.
15. Gottlow J, Johansson C, Albrektsson T, Lundgren AK. Biomechanical and histologic evaluation of the TiUnite and Osseotite implant surfaces in rabbits after 6 weeks of healing. Appl Osseointegration Res 2000; 1:25–27.
16. Ivanoff C-J, Widmark G, Johansson C, Wennerberg A. Histologic evaluation of bone response to oxidized and turned titanium micro-implants in human jawbone. Int J Oral Maxillofac Implants 2003; 3:341–348.
17. Zechner W, Tangl S, Fürst G, et al. Osseous healing characteristics of three different implant types. A histologic and histomorphometric study in mini-pigs. Clin Oral Implants Res 2003; 14:150–157.
18. Rocci A, Martignoni M, Burgos P, Gottlow J, Sennerby L. Histology of retrieved immediately and early loaded oxidized implants. Light microscopic observations after 5 to 9 months of loading in the posterior mandible of 5 cases. Clin Implant Dent Relat Res 2003; 5(Suppl 1):88–98.
19. Donath K, Breuner G. A method for the study of undecalcified bones and teeth with attached soft tissues. The Säge-Schliff (sawing and grinding) technique. J Oral Pathol 1982; 11:318–326.
20. Bobyn JD, Pilliar RM, Cameron HU, Weatherly GC. The optimum pore size for the fixation of porous surfaced metal implants by the ingrowth of bone. Clin Orthop Relat Res 1980; 150:263–270.
21. Clemow AJT, Weinstein AM, Klawitter J, Koeneman J, Andersson J. Interface mechanics of porous titanium implants. J Biomed Mater Res 1981; 15:73–82.
22. Kokubo T, Kim HM, Kawashita M, Nakamura T. Bioactive metals: preparation and properties. J Mater Sci Mater Med 2004; 15:99–107.
23. Glauser R, Ruhstaller P, Windisch S, et al. Immediate occlusal loading of Brånemark System® TiUnite™ implants placed predominantly in soft bone: 4-year results of a prospective clinical study. Clin Implant Dent Relat Res 2005; 7(Suppl 1):52–59.
24. Glauser R, Lundgren AK, Gottlow J, et al. Immediate occlusal loading of Brånemark MkIV TiUnite™ implants placed predominantly in soft bone: 1-year results of a prospective, clinical study. Clin Implant Dent Relat Res 2003; 5(Suppl 1):47–56.
25. Calandriello R, Tomatis M, Vallone R, Rangert B, Gottlow J. Immediate occlusal loading of single lower molars using Brånemark System Wide Platform TiUnite implants: an interim report of a prospective, open-ended clinical multicenter study. Clin Implant Dent Relat Res 2003; 5(Suppl 1): 74–80.
26. Vanden Bogaerde L, Pedretti G, Dellacasa P, Mozzati M, Rangert B. Early function of splinted implants in maxillas and posterior mandibles using Brånemark System TiUnite implants: an 18-month prospective clinical multicenter study. Clin Implant Dent Relat Res 2004; 6:121–129.
27. Rocci A, Martignoni M, Gottlow J. Immediate loading of Brånemark System with TiUnite and machined surfaces in the posterior mandible: a randomised, open-ended trial. Clin Implant Dent Relat Res 2003; 5(Suppl 1):57–63.
28. Glauser R, Ree A, Lundgren A, Gottlow J, Hammerle CH, Scharer P. Immediate occlusal loading of Brånemark implants applied in various jawbone regions: a prospective, 1-year clinical study. Clin Implant Dent Relat Res 2001; 3:204–213.